Removal of perfluorooctane sulfonate by a gravity-driven membrane: Filtration performance and regeneration behavior

Hao Guo, Jianqiang Wang, Ye Han, Yong Feng, Kaimin Shih, Chuyang Y. Tang*

Department of Civil Engineering, The University of Hong Kong, Pokfulam, Hong Kong

*Corresponding Author:

Chuyang Y. Tang, tangc@hku.hk, +852 28591976

Abstract

Perfluorooctane sulfonate (PFOS) has been under the spotlight in recent decades due to its adverse environmental and ecological concerns. Existing treatment methods (such as reverse osmosis and nanofiltration) for this recalcitrant surfactant are generally energy intensive. In this study, for the first time, a gravity-driven filtration using a highly porous nanofibrous membrane was systematically investigated for PFOS removal. The membrane possesses a high water permeability of 354.9 LMH/kPa, allowing the membrane to be operated under gravity-driven conditions. PFOS removal efficiency ranging from 36-90% was observed under a wide range of water chemistry conditions (5-20 ppb PFOS, pH 4-10, and ionic strength 1-10 mM). The best removal efficiency was obtained at pH 4 and 10 mM ionic strength as a result of the enhanced PFOS-membrane electrostatic attraction and/or weakened electrostatic repulsion. The removal efficiency was also higher at lower membrane permeate flux due to the increased residence time of PFOS molecules in the internal pores of the membrane. Simple methanol rinsing was able to effectively regenerate the membrane, and the high PFOS removal efficiency can be maintained over 20 cycles of regeneration. The current study may provide important insights of using highly porous membranes for energy-efficient PFOS removal and recovery.

Key Words

Perfluorooctane sulfonate (PFOS), nanofibrous membrane, gravity-driven filtration, removal,

regeneration

1. Introduction

Perfluorooctane sulfonate (PFOS), a surfactant whose eight-carbon chain is completely fluorinated, has caused environmental and ecological concerns globally in recent decades [1-4]. It has been widely used for manufacturing various products such as fighting foams, coatings and semi-conductors for many decades [5, 6]. In 2002, PFOS was classified as a toxic pollutant by Organization for Economic Co-operation and Development [7] owning to the increasing evidence of its bioaccumulation [8] and toxicity (e.g., developmental toxicity [9], hepatotoxicity, and carcinogenicity [10-12]). This action was quickly followed by a wave of directives and regulations to ban or restrict the use of PFOS by many countries and regions [13-15]. Nevertheless, PFOS is still detected at noticeable concentrations (ng/L to μg/L) in the environment [16-19], and it will likely remain in the environment for a long time due to its persistent nature (estimated half-life > 41 years in water [20]).

Since a major pathway for PFOS entering water system is through wastewater discharge [21], removal of PFOS during wastewater treatment is of critical importance. However, because of its resistance to enzyme attack, PFOS is highly recalcitrant to typical biological wastewater treatment processes such as activated sludge treatment and anaerobic digestion [22-24]. Various approaches were investigated to treat PFOS-containing wastewater in recent years, for instance, sonochemical degradation [25], photochemical degradation [26], electrochemical oxidation [27], adsorption [28], ion-exchange [29] and membrane separation [30]. Among

them, membrane separation stands out as an effective way for PFOS removal. Generally, high retention membranes such as reverse osmosis (RO) and nanofiltration (NF) are used. NF can generally achieve > 90% of PFOS rejection [30, 31], while RO presents rejection as high as ≥ 99% [30, 32]. Nevertheless, NF and RO are generally energy intensive since relatively high pressure is needed to drive these membrane processes (e.g., a few hundreds kPa for NF and > 1000 kPa for RO [33]).

In contrast to dense RO and NF membranes, nanofibrous membranes are a type of highly porous membranes with large internal porosity and surface area as well as low hydraulic resistance [34]. For these reasons, these novel membranes have attracted increasing attention for potential environmental applications such as low-energy filtration [35]. Meanwhile, compared to other low-energy filters (e.g., polymeric microfiltration membranes or glass fiber filters), nanofibrous membranes present much larger internal surface area to capture environmental pollutants (e.g., disinfection by-products [36] and heavy metals [37, 38]). In addition, it is also likely to use such large internal surface area to conduct further surface modification for enhanced contaminants removal. Thus, nanofibrous membranes can potentially offer a low-energy removal option for treating PFOS. A post-treatment step can be further designed to regenerate the pollutant-laden membranes and to recover PFOS from wastewater. To the best knowledge of the authors, the application of nanofibrous membranes

for PFOS-containing water treatment has never been reported in the literature.

The purpose of this study was to investigate PFOS removal by nanofibrous membranes and membrane regeneration. A commercial nanofibrous membrane was used to remove PFOS under gravity-driven conditions for the first time. The effect of water chemistry (PFOS concentration, pH and ionic strength) and other operational conditions on removal efficiency was studied systematically. Membrane regeneration and PFOS recovery were achieved by a simple methanol elution step. This study may provide a highly energy-efficient alternative method for PFOS removal and recovery.

2. Materials and methods

2.1 Chemicals. PFOS was purchased from Sigma-Aldrich (St. Louis, MO) in the form of potassium salt (≥ 98%). The physicochemical properties of PFOS was presented in Appendix A. Analytical grade sodium chloride (BDH, Dorset, UK), sodium hydroxide (BDH, Dorset, UK) and hydrochloride acid (37 wt.%, VWR, Dorset, UK) were used to adjust solution chemistry (ionic strength and pH). Optima grade methanol (Fisher Scientific, Pittsburgh, PA) was used for PFOS analysis in LC/MS/MS system and for membrane regeneration. Ultrapure water was provided by the Milli-Q water system (Millipore, Billerica, MA).

2.2 Membrane and characterization. A commercial flat-sheet nanofibrous membrane was obtained from Ahlstrom Corp. (Disruptor®, Helsinki, Finland). According to the manufacturer, the membrane was consisted of inorganic mineral nanofibers coated on glass fibers, which are further reinforced by non-woven fabric supports. In the current study, membrane pure water permeability was tested using ultrapure water under constant gravitational driving force using the setup shown in Figure B1 (Appendix B). Other physiochemical properties (morphology, surface area, chemical composition, crystalline structure, and wettability) of the membrane were systematically characterized. Before analysis, all the samples were cleaned by rinsing and soaked in ultrapure water for at least 24 hours and dried at room temperature in air.

The membrane morphology was imaged by a field-emission scanning electron microscope (FE-SEM, Hitachi S-4800, Japan). Before imaging, dried membrane samples were sputter-coated with a thin layer of gold by a sputter coater (BAL-TEC SCD 005, Liechtenstein). SEM micrographs were scanned at an acceleration voltage of 5 kV. In addition, elemental information was obtained by an energy dispersive X-ray detector (EDX, Horiba EMAX, Japan) equipped in the FE-SEM.

The crystalline phase information of the membrane was determined by X-ray diffraction (XRD) using a D8 Advance Diffractometer (Bruker AXS, Billerica, MA). The XRD was

equipped with a Cu X-ray tube operated at 40 kV and 40 mA. Scan was conducted from 10° to 80° 2θ-angle with a sampling time of 0.2 s per step. Attenuated total reflectance Fourier transform infrared spectroscopy (ATR-FTIR) was performed on a Spectrum 100 FT-IR Spectrometer (Perkin Elmer, Waltham, MA). The scan was operated with a wavenumber range from 650 to 4000 cm^{-1}. The contact angle of the membrane was tested on a Contact Angle Analyzer (Powereach®, China) by the sessile drop method. The reported contact angle is the average value of ten replicates. The total membrane surface area (including internal pore surface area) was determined by a BET surface area analyzer (Beckman Coulter SA 3100, Fullerton, CA).

2.3 PFOS removal experiments. PFOS removal was performed in a stirred membrane cell (Model 8400, Millipore, Billerica, MA) at room temperature (24 °C) under gravity-driven conditions. For each filtration experiment, two new disk coupons of the nanofibrous membrane (diameter = 7.6 cm) were mounted in the cell. A 350 mL solution containing a predetermined concentration of PFOS (5 ~ 20 ppb) was added into the cell, and gentle stirring was performed throughout the filtration experiment. Solution pH (pH 4, 7, and 10) and ionic strength (1 mM and 10 mM) were carefully controlled by the addition of sodium hydroxide, hydrochloric acid, and/or sodium chloride in order to investigate the effect of water chemistry on PFOS removal efficiency. The weight of permeate water was measured by a digital balance

to determine the water flux. Samples were collected from both the cell and the permeate simultaneously at specific time intervals for PFOS analysis.

The total volume of the solution flowing through the membrane is defined as volumetric load (L/m^2) and calculated by:

$$\text{Volumetric load} = \frac{\text{Permeate volume treated by the membrane}}{\text{Effective membrane area}} \quad (1)$$

The PFOS load ($\mu g/m^2$) can be similarly defined as the total mass of the contaminant that the membrane has been subjected to:

$$\text{PFOS load} = \frac{\text{PFOS mass treated by the membrane}}{\text{Effective membrane area}} \quad (2)$$

The removal efficiency of the membrane can then be calculated by:

$$\text{Efficiency} = 1 - \frac{\text{Total mass of PFOS measured in the permeate}}{\text{PFOS load} \times \text{Effective membrane area}} \quad (3)$$

PFOS static adsorption experiments were conducted in a 600 mL polypropylene (PP) container containing two new disk coupons of nanofibrous membrane (diameter = 7.6 cm) and 350 mL PFOS solution with different concentration from 5 ppb to 500 ppb (pre-adjusted pH of 7.0 and ionic strength of 10 mM NaCl). All containers were shaken with moderate speed at room temperature (24 °C) for at least 72 h. Then Samples were taken for PFOS analysis.

2.4 Membrane regeneration. In the regeneration experiments, a 250 mL PFOS solution with

an initial concentration of 10 ppb, pH of 7.0 and ionic strength of 10 mM was added into the cell and the permeate was collected. Subsequently, 10 mL methanol was used to regenerate the membrane. After a brief water-rinsing step, the above procedures were repeated for a total of 20 cycles in order to investigate the regeneration behavior of the membrane upon repeated usage. Samples from the cell (feed), permeate and methanol-eluted solution were taken for PFOS analysis. All the experiments were triplicated.

2.5 PFOS quantification. Details about PFOS analytical method can be found in our previous work [39]. Briefly, the PFOS samples were diluted with methanol at a water/methanol volume ratio of 50%/50%. The methanol diluted samples were filtrated through a 0.2 μm Whatman inorganic syringe filter (Maidstone, UK), and the filtrate was collected in a 1.5 mL amber vial. Analysis was performed by a UPLC/MS/MS system equipped with a 50 × 2.1 mm BEH C18 column with 1.7μm particle size and tandem quadrupole mass spectrometers (Waters, Milford, MA). A MS/MS scan was operated in electrospray negative ionization mode to analyze PFOS under the specific transition (*m/z*) of 499/80. The details of instrumental detection dynamic range was reported in Appendix C.

3. Results and Discussions

3.1 Membrane characterization. Visual observation revealed that the membrane has a

multi-layered sandwiched structure. The overall thickness is approximately 1 mm. The multi-layered structure is confirmed by SEM observation (Figures 1a,b). SEM micrographs show a highly porous nanofibrous membrane mat (see Figure 1b) covered by a layer of larger-diameter fibers (~ 20 μm in diameter, Figure 1a) on each side. Based on the manufacturer's information, this layer is a non-woven fabric for supporting the nanofibers. According to BET analysis, the nanofibrous membrane had a relatively large BET surface area of 28.1 ± 0.3 m^2/g, which may potentially provide abundant sites for PFOS uptake.

EDX analysis (Figures 1c-f) revealed that the larger-diameter fibers are mainly composed of carbon and oxygen, and that the nanofibers mainly contain aluminum, silica and oxygen. The EDX results are consistent with manufacturer's information that the nanofibrous membrane was made by growing aluminum oxide on a glass fiber substrate. Further material characterization was performed using XRD and ATR-FTIR. XRD results (Figure 2a) indicated boehmite [AlO(OH)] and silicon oxide [SiO_2] as the main crystalline phases in the membrane. These crystalline phases can be assigned to the nanofibrous mat: the membrane with the non-woven fabrics peeled away (i.e., the nanofibrous mat) showed clearly identifiable FTIR peaks (Figure 2b) corresponding to Al-O stretching (1061 cm^{-1}) [40] and Si-O-Si bending (882 cm^{-1}) [41]. In contrast, the intact membrane had major peaks at 1713 cm^{-1}, 1240 cm^{-1}, 1092 cm^{-1}, and 722 cm^{-1} (Figure 2b), which can be attributed to poly(ethylene terephthalate)

or PET [42], a common material for nonwoven fabrics [43]. The membrane had a relatively high contact angle of 115.0 ± 2.3°, which may be attributed to the hydrophobic nature of PET. Upon peeling away the PET non-woven fabric cover, the remaining membrane can be spontaneously wetted by water.

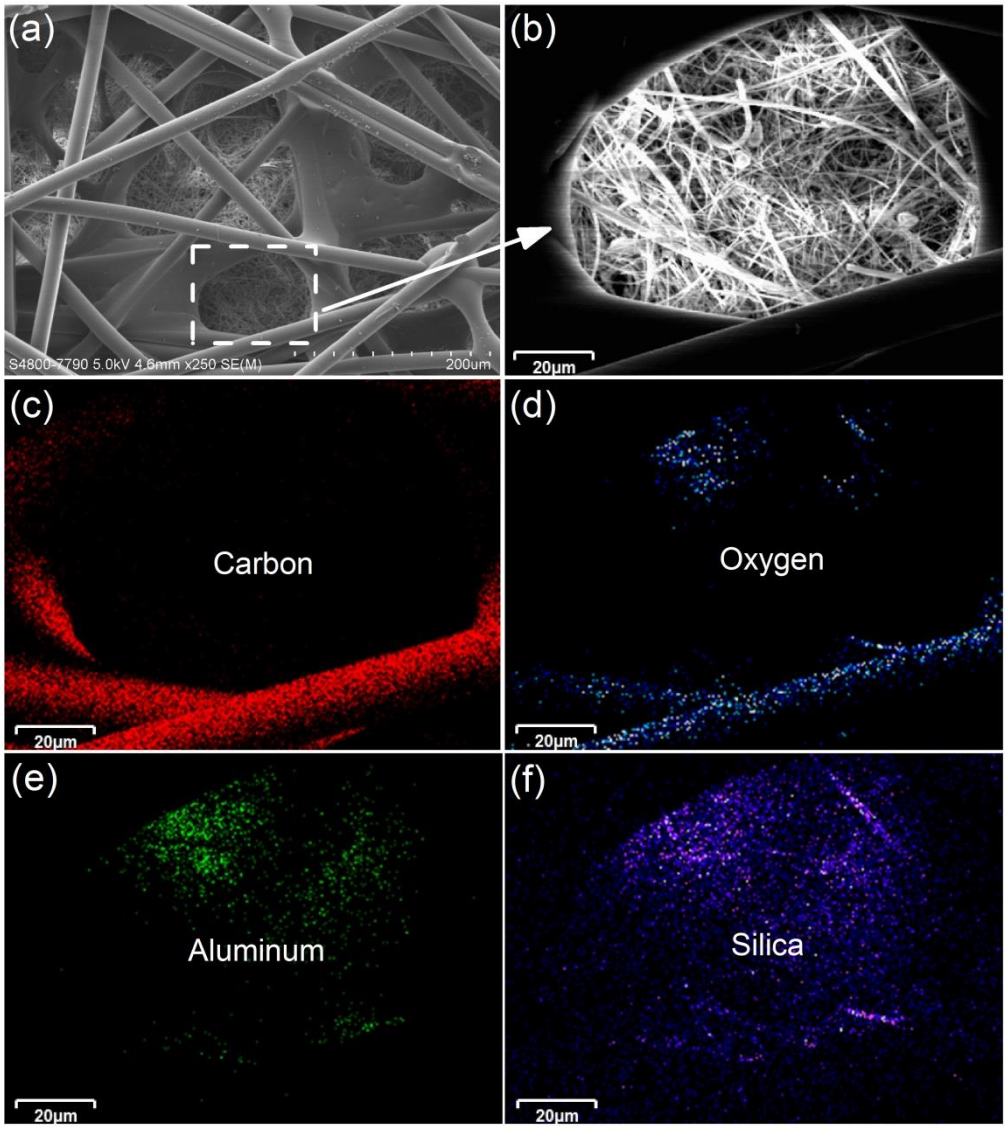

Figure 1. SEM images and EDX elemental analysis of the nanofibrous membrane. SEM micrographs were obtained at two different magnifications (a: scale bar = 200 μm; b: scale bar = 20 μm). EDX analysis were performed to obtain the elemental mapping of carbon (c), oxygen (d), aluminum (e), and silica (f). Since EDX is not able to detect hydrogen, hydrogen is not included in the EDX elemental analysis.

The pure water permeability of the membrane was tested under gravity-driven conditions (Figure 3). A high water flux of 345.2 L/m^2.h (LMH) was obtained with a merely 10-cm water head (i.e., a pressure difference of 0.98 kPa). The membrane had a water permeability of 354.9 LMH/kPa. In comparison, commercial RO and NF membranes have typical water permeability values ranging from 0.01-0.08 and 0.08-0.2 LMH/kPa, respectively [44, 45]. The high permeability can be attributed to the great internal porosity and the excellent wettability of the nanofiber mat, which enables the membrane to be potentially used for low energy (e.g., gravity-driven) membrane filtration.

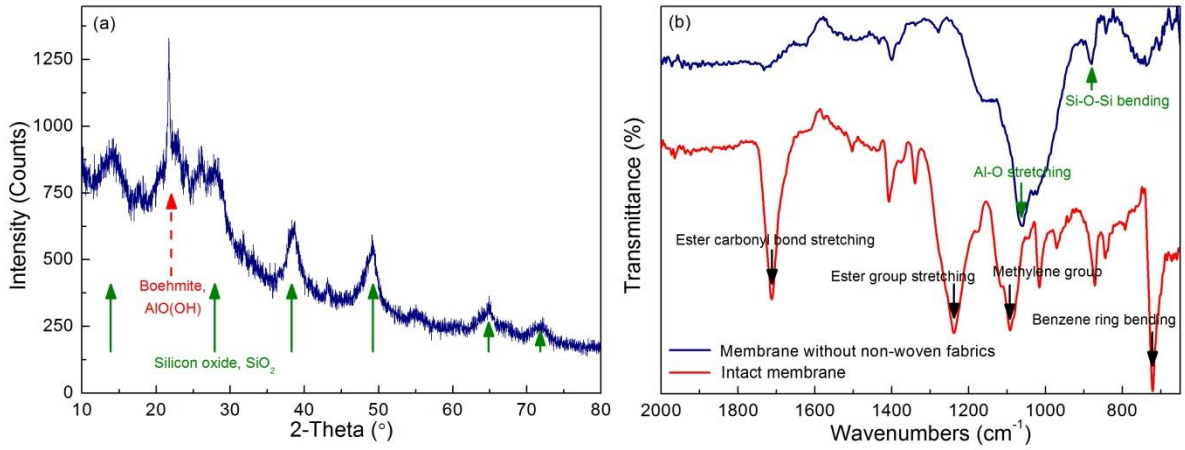

Figure 2. XRD and FTIR results. (a) XRD spectrum of the nanofibrous membrane without non-woven fabrics, (b) ATR-FTIR spectra of the nanofibrous membrane with and without non-woven fabrics.

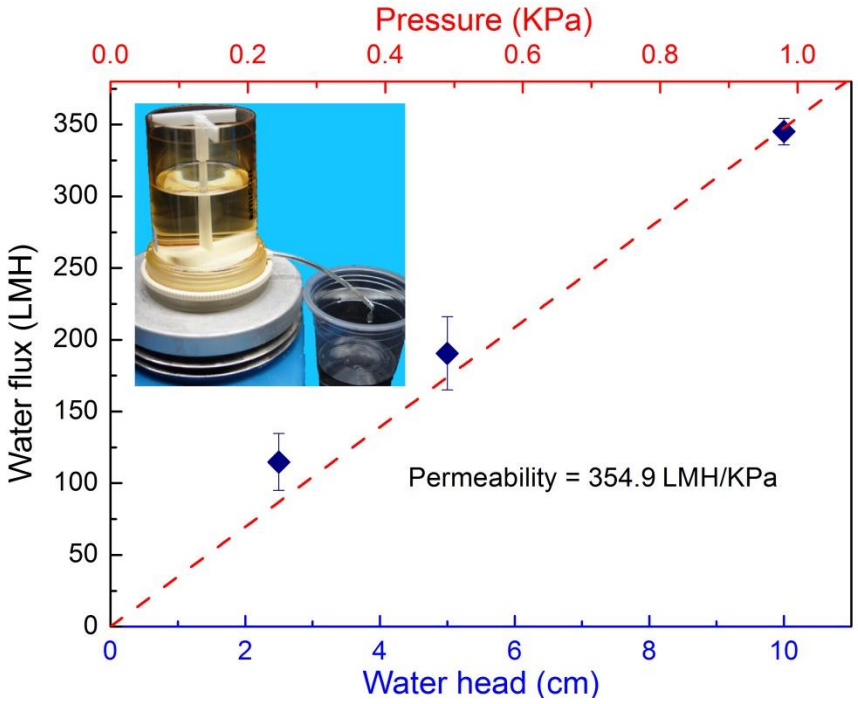

Figure 3. Membrane permeate flux as a function of water head (and applied pressure). Ultrapure water was used as the feed solution. The tests were performed under constant water head (2.5, 5.0, or 10.0 cm).

3.2 Effects of water chemistry. The effects of various water chemistry conditions (PFOS concentration, pH and ionic strength) are presented in Figures 4 and 5. Generally, greater amount of PFOS was removed for higher feed concentration under identical volumetric load (Figure 4a). Nevertheless, a better way to compare PFOS removal is to normalize the removal against the mass of PFOS loaded to a unit membrane area. In Figure 4 (b), PFOS removal is plotted as a function of PFOS load for the three different feed concentrations (5, 10, and 20 ppb). Interestingly, the three removal curves were nearly collapsed into a single one, which suggests PFOS load instead of feed concentration as the most important variable determining the amount of removal.

The plot in Figure 4(b) further allows one to obtain the removal efficiency at different PFOS load, where the dashed line with a slope of 1 represents a removal efficiency of 100%. Thus, data points falling on this line indicate a complete removal. On the other hand, data points far below the line imply poor removal efficiency. From Figure 4(b), the initial PFOS removal was nearly 100% at PFOS load of less than 100 $\mu g/m^2$. The removal efficiency decreased significantly at higher PFOS load. Since the nanofibrous membrane in the current study does not present a dense rejection layer, PFOS removal is mainly by adsorption (in contrast to size exclusion for the case of RO [32], adsorption isotherms were given in Appendix D). Thus, the greater removal efficiency at lower PFOS load is likely attributed to free availability of adsorption sites at the initial filtration stage. As filtration progresses, these sites are gradually occupied to cause a reduced removal efficiency. Among the three PFOS concentrations tested in the current study (5 – 20 ppb), the adsorption capacity under higher feed concentration appears to be consumed much faster at identical volumetric load, implying great volume of water can be treated for feed solutions containing relatively low PFOS concentrations [46].

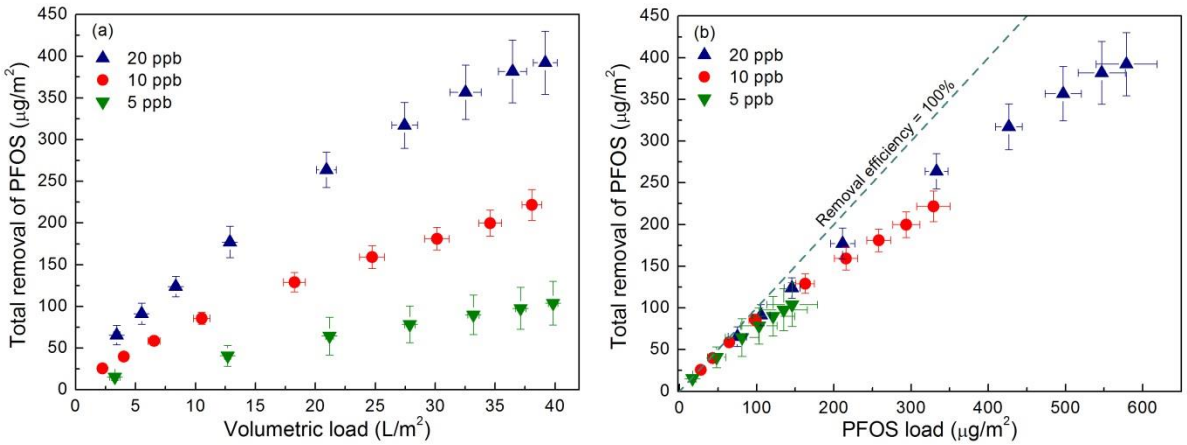

Figure 4. PFOS removal as a function of volumetric load (a) and mass load (b) at different feed water concentrations. Experimental conditions: feed volume of 350 mL, pH 7.0, 10 mM NaCl and water flux of 69 ± 2.3 L m^{-2} h^{-1}.

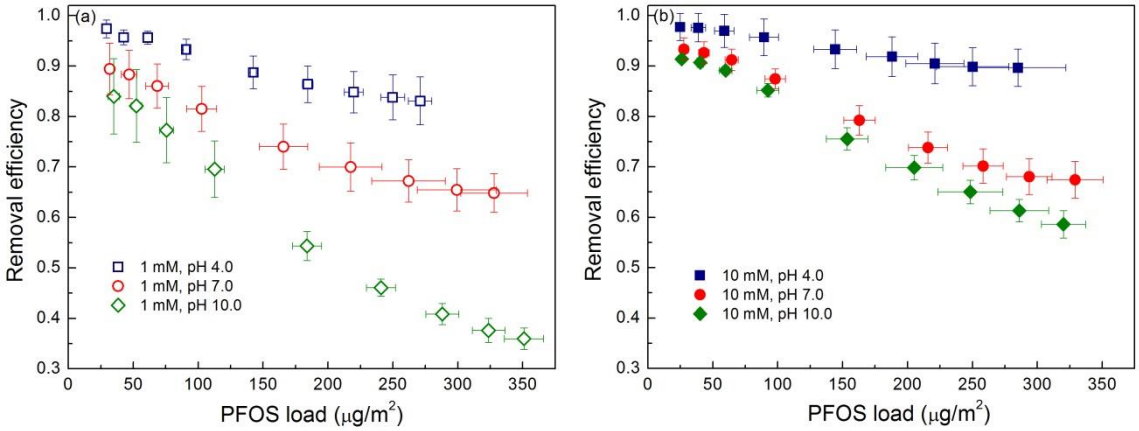

Figure 5. Effect of water chemistry on PFOS removal efficiency in 1 mM NaCl (a) and 10 mM NaCl (b). Other experimental conditions: feed volume of 350 mL, 10 ppb PFOS and water flux of 69 ± 2.3 L m^{-2} h^{-1}.

The removal of PFOS by the nanofibrous membrane is significantly affected by both pH and ionic strength (Figure 5). Clearly, PFOS removal was enhanced at lower pH and higher ionic strength. These effects can be readily explained by the electrostatic interaction between PFOS and the membrane. The nanofibrous membrane mainly consists of PET cover, boehmite, and silicon oxide (Figure 2), although the PET cover barely contributed to PFOS removal (Appendix E). Both boehmite (pH_{PZC} = 8.4) [47] and silicon oxide (pH_{PZC} ~ 2 - 3) [48]

become more positively charged (or less negatively charged). The result of membrane zeta potential also reveals its positively charged nature under lower pH (Appendix F). Since PFOS presents as an anion due to its low pKa (< 0) [7], reducing pH enhances the PFOS-boemite electrostatic attraction [47] and weakens the PFOS-silicon oxide electrostatic repulsion [49] to promote greater PFOS adsorption. Meanwhile, increasing ionic strength has the effect to suppress the electrostatic repulsion between PFOS anions, resulting in increased adsorption onto the membrane. The current results are consistent with the existing literature on PFOS adsorption by mineral surfaces: Tang et al. [49] reported that both increasing ionic strength and reducing pH increased PFOS uptake by goethite (and silicon oxide to a lesser degree) due to their effects regulating PFOS-PFOS and PFOS-mineral electrostatic interactions.

3.3 Effects of operational conditions. Water flux is an important parameter in filtration process, since it is closely related to membrane productivity as well as energy consumption of the process. In the current study, PFOS removal decreased when increasing flux from 38 to 158 LMH (Figure 6). This observation is in apparent contradiction with the typical trend of increased rejections for RO and NF membranes at higher water flux [30]. In the latter case, rejection are improved by the dilution mechanism: solutes and water molecules diffuse through a dense rejection layer of RO or NF membrane independent of each other, and great water flux tends to dilute the contaminant concentration in the permeate water [50]. In

contrast, solutes pass through the porous nanofiberous membrane by convection. A greater water flux generally means shorter residence time of PFOS molecules in the membranes, which explains the decreased adsorption efficiency.

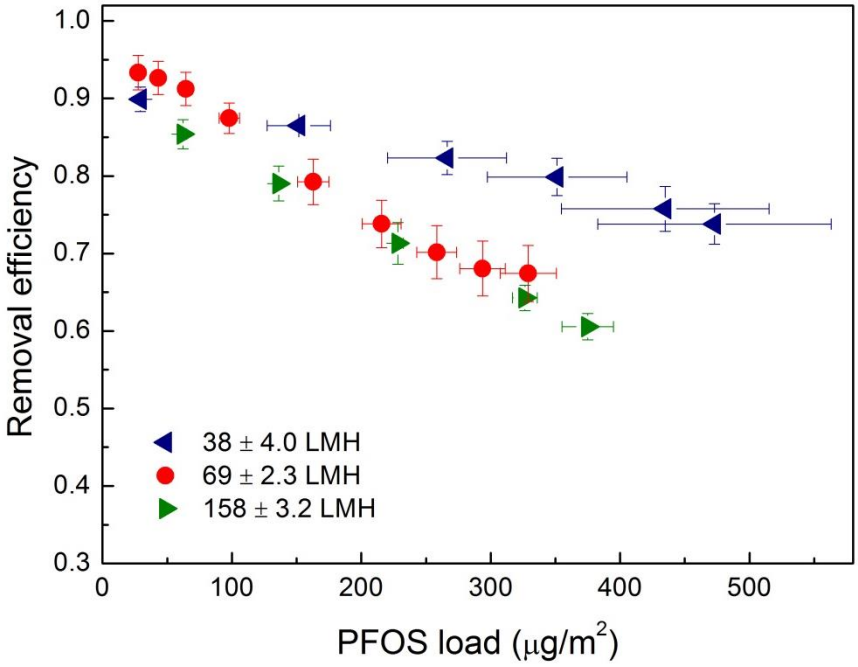

Figure 6. Effect of different water flux on PFOS removal efficiency. Experimental conditions: feed volume of 350 mL, 10 ppb PFOS, pH 7.0 and 10 mM NaCl.

An additional two-pass filtration experiment was performed, where the PFOS-containing permeate water was filtrated through a second pass membrane (clean membrane coupon) to simulate multi-pass filtration conditions that aimed to further improve removal. Under the identical water chemistry conditions (10 ppb PFOS in the feed, pH 7, 10 mM NaCl), the two-pass filtration achieved a significantly higher removal efficiency of 82.0 ± 7.8 % compared to the single-pass efficiency of 63.2 ± 9.4 %. The two-pass arrangement effectively prolongs the residence of PFOS molecules in the membranes, leading to the enhanced

removal by adsorption. Alternatively, the removal efficiency of a *n*-pass filtration η_n may be estimated by a filtration-in-series model: $1 - \eta_n = (1 - \eta_1)^n$, where stands for the single-pass efficiency. The η_2 value estimated from the above model is 86.5%, which agrees reasonably well with the experimental value.

3.4 Membrane regeneration. Since PFOS removal by the nanofibrous membrane is by adsorption, membrane regeneration is critical to ensure its repeated use upon the saturation of the membrane adsorption capacity. In the current study, membrane regeneration was achieved by a simple methanol rinsing step (Section 2.4). In the literature, methanol has been commonly used to prevent PFOS loss from solution due to adsorption and as a solvent for PFOS elution during solid phase extraction [51]. Therefore, methanol is expected to be a good candidate for PFOS extraction from the exhausted nanofibrous membrane. The recovery ratio of PFOS by methanol rinsing was 112.4% ± 11.8%, implying methanol is effective for PFOS regeneration. Figure 7 shows that the regenerated nanofibrous membrane was able to maintain high removal efficiency (~ 85%) for PFOS even after 20 cycles regeneration. This result indicates that the nanofibrous membrane was robust against the regeneration procedures. Nevertheless, we observed improved removal efficiency over the first five cycles of regeneration. While the exact reason of such behavior is not known, it is suspected that the methanol rinsing helps to remove some impurities that may otherwise compete for adsorption

sites, which results in reduced removal efficiency. To further understand this effect, we compared the PFOS removal of three clean membranes with different pretreatment steps: (1) ultrapure water rinsing, (2) 10 ml methanol rinsing followed by ultrapure water rinsing, and (3) 50 ml methanol rinsing followed by ultrapure water rinsing. Appendix G Figure G1 clearly shows that the methanol pretreated membranes showed better PFOS removal, consistent with the trend observed in Figure 7.

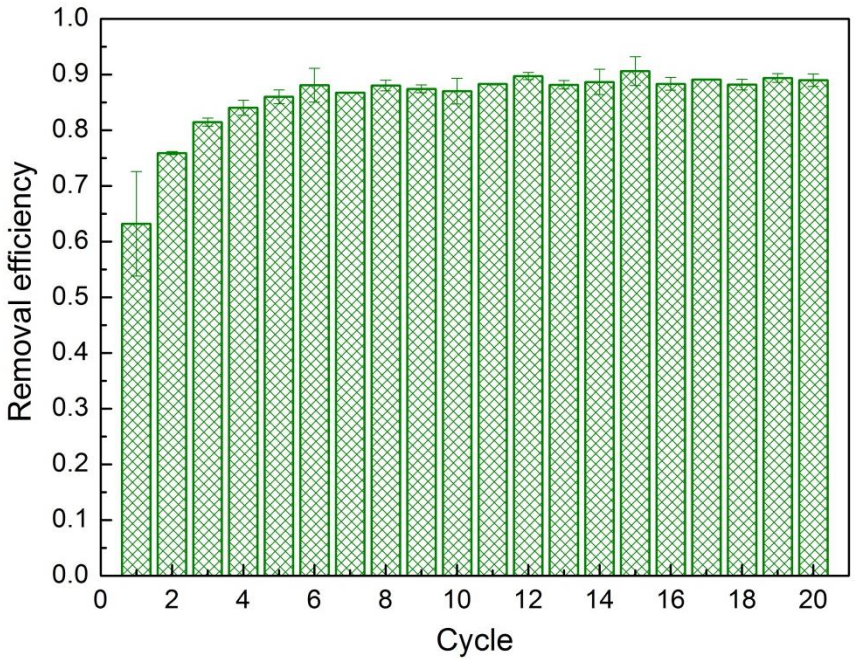

Figure 7. Regeneration behavior of the nanofibrous membrane by methanol rinsing in multiple cycles.Filtration experimental conditions: feed volume of 250 mL, 10 ppb PFOS, pH 7.0 and 10 mM NaCl. Regeneration experimental conditions: 10 ml methanol rinsing followed by ultrapure water rinsing.

3.5 Implication. Although the nanofibrous membrane was primarily applied for PFOS removal, the membrane can in principle be applied for treating other types of contaminants

such as heavy metals and trace organic pollutants. Future investigations may further explore surface modifications of the nanofibers to further enhance contaminant removal efficiency. The membrane's ability for gravity-driven operation (thus avoiding the need of electricity supply) may also allow it to be used for disaster relief in emergency situations as well as water treatment in developing countries.

4. Conclusions

In the current study, a boehmite-silica based nanofibrous membrane was applied to remove PFOS from water solution with different pH (4-10) and ionic strength (1 and 10 mM). Due to the highly porous nature of the membrane, relatively high water flux was obtained under gravity-driven conditions. Meanwhile, significant PFOS removal was observed, particularly under lower pH and higher ionic strength conditions. Under these conditions, the enhanced PFOS-membrane electrostatic attraction and/or weakened electrostatic repulsion favors the adsorption of PFOS by the membrane. Furthermore, the membrane can be easily regenerated with a simple methanol rinsing step and high efficiency was maintained over 20 cycles of regeneration. Thus, the boehmite-silica nanofibrous membrane provides a highly energy-efficient and viable alternative treatment option for removing the recalcitrant perfluorinated surfactant from PFOS-containing wastewater. Compared to conventional RO and NF treatment that requires applied pressures on the order of 1000 kPa , the nanofibrous

membrane used in the current study can be operated with a pressure as low as 0.98 kPa (i.e., 10 cm water head). Indeed, the ability for efficient PFOS recovery and membrane regeneration may further allow this membrane to be applied for PFOS extraction (e.g., from semiconductor wastewater containing high PFOS concentration) to enable its subsequent reuse.

Acknowledgements

The study is supported by the Seed Funding for Basic Research (Project number 104002660) at the University of Hong Kong and General Research Fund (Project number 17207514) by the Research Grants Council of Hong Kong. Hao Guo receives a Postgraduate Scholarship from the University of Hong Kong. The authors thank the financial support from the Strategic Research Theme (Clean Energy) at the University of Hong Kong. Ahlstrom Corp. is thanked for providing the membrane samples. Dr. Tong Zhang and Miss Yu Deng are thanked for their kind help on UPLC-MS/MS operation.

Appendix A. Physicochemical properties of PFOS

Table A1. Physicochemical properties of PFOS [52]

Compound	Formula	Molecular Weight	pKa	Log Kow
PFOS (potassium salt)	$CF_3(CF_2)_7SO_3K$	538	< 0	Not measurable

Appendix B. Membrane pure water permeability tests

Figure B1 shows the filtration setup designed to achieve a constant water head. Overflow tubes (diameter of 2.5 mm) were inserted at 2.5, 5.0 and 10.0 cm for controlling water head. A peristaltic pump was used for refilling purpose where necessary. Permeate water was collected at predetermined time, and the weight of the water was used for membrane water flux calculation. All tests were conducted in triplicate, and new membrane was used in each test.

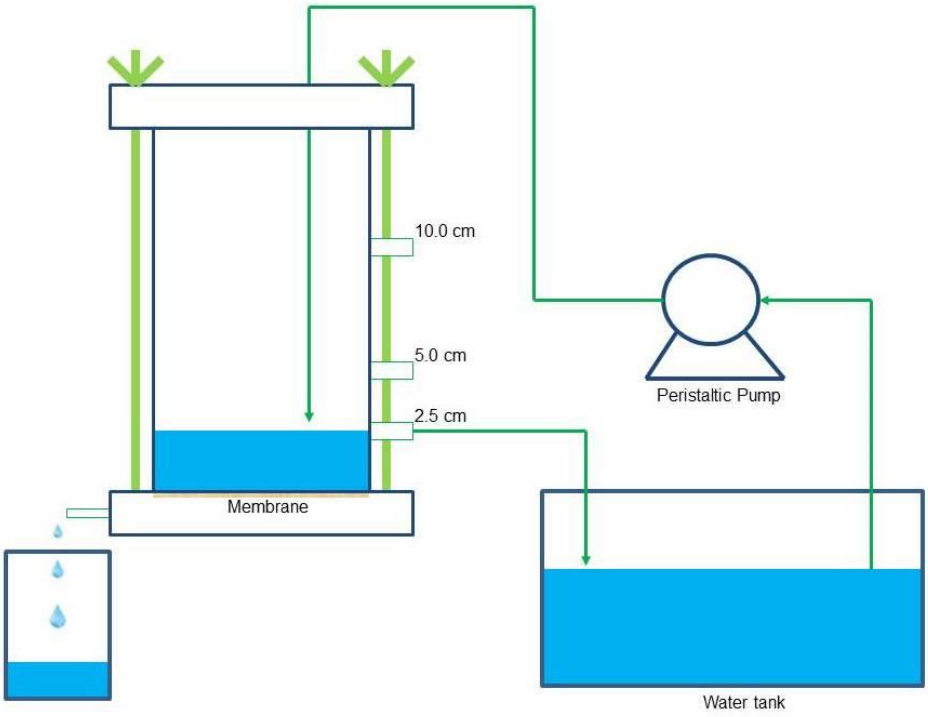

Figure B1. Membrane pure water permeability test setup

Appendix C. Dynamic range of PFOS detection.

A serial calibration points (0.5 – 30 ppb) were used to calibrate the concentration of PFOS. The dynamic range from the lowest calibration point (i.e. 0.5 ppb) to the highest calibration point (i.e. 30 ppb) gave a good fit with linearity over 0.999 (Figure C1). PFOS concentration used in this study was covered by this range. Meanwhile, the lowest calibration concentration of 0.5 ppb showed a signal-to-noise (S/N) ratio above 10:1, which is considered as a critical value of instrumental quantification limit (IQL).

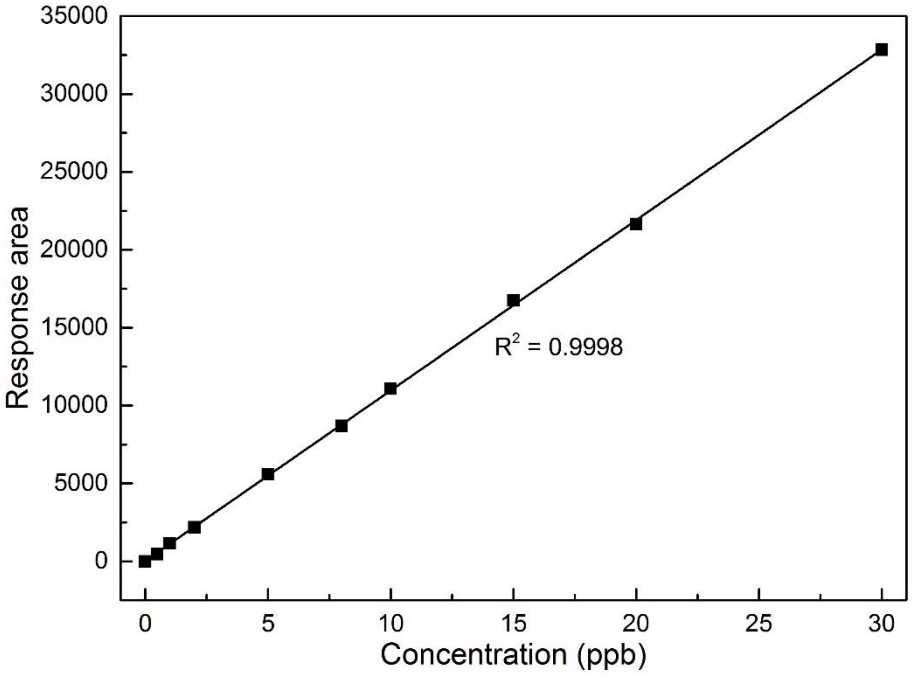

Figure C1. Dynamic range of PFOS detection by UPLC-MS/MS.

Appendix D. Adsorption isotherms

Figure D1 gives the simulation results of PFOS adsorption on the nanofibrous membrane by Langmuir and Freundlich model. Details of two isotherms can be found in published literatures [53, 54]. The experimental results fitted both well with Langmuir and Fredunlich model (both correlation coefficient $R^2 > 0.99$). The good fitting of Langmuir model suggests

that PFOS adsorption on the nanofirous membrane might be a monolayer interaction. The good fitting of Freundlich model hints that PFOS-PFOS interaction might be responsible for the nonlinear isotherm (n = 1 represents linear isotherm) [28]. The simulated results of q_m and K_F suggests the potential of this nanofibrous membrane for PFOS removal.

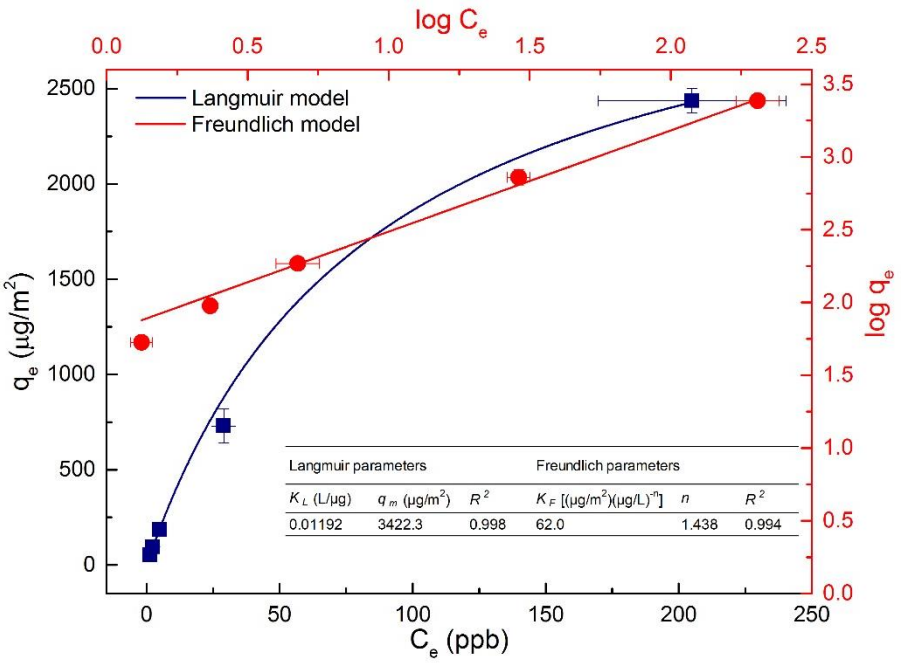

Figure D1. PFOS adsorption isotherms onto the nanofibrous membrane. q_e is the PFOS amount adsorbed on the nanofibrous membrane (μg/m^2), C_e is the PFOS concentration in solution (ppb), K_L is the Langmuir adsorption conatant (L/μg), q_m is the maximum sorption capacity (μg/m^2), K_F is the Freundlich adsorption conatant related to sorption capacity [(μg/m^2)(μg/L)$^{-n}$], and n is a conatant of sorption intensity. Experimental condition: solution volume of 350 mL, 5-500 ppb PFOS, pH 7.0 and 10 mM NaCl.

Appendix E. Effect of PET cover on PFOS removal

Figure E1 presents the PFOS removal efficiency by intact nanofibrous membrane and PET cover peeled off from the membrane. Clearly, the PET cover had negligible effect on PFOS removal efficiency compared to the intact nanofibrous membrane.

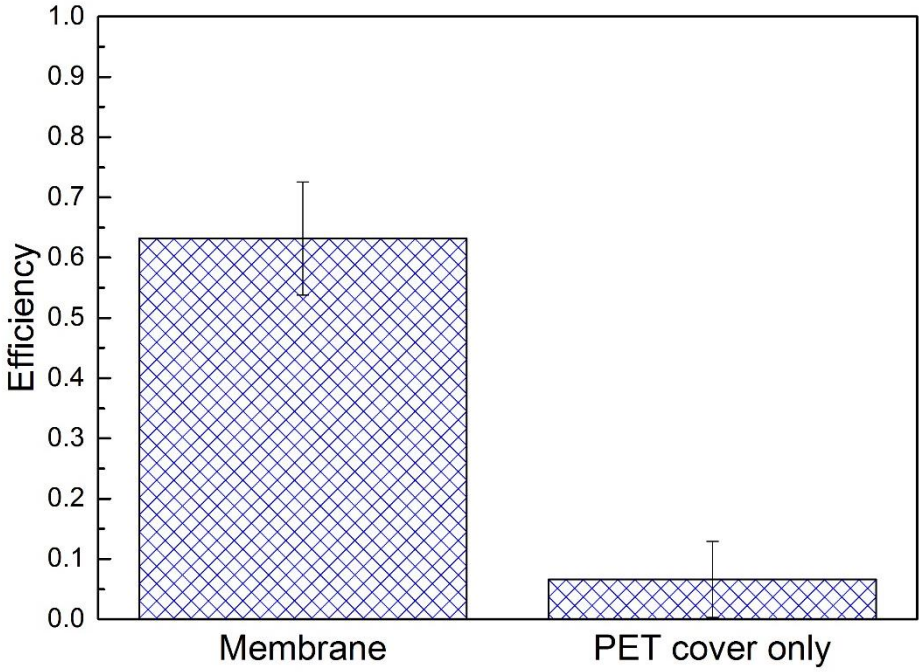

Figure E1. PFOS removal by intact nanofibrous membrane and PET cover. Experimental condition: solution volume of 250 mL, 10 ppb PFOS, pH 7.0 and 10 mM NaCl.

Appendix F. Membrane zeta potential

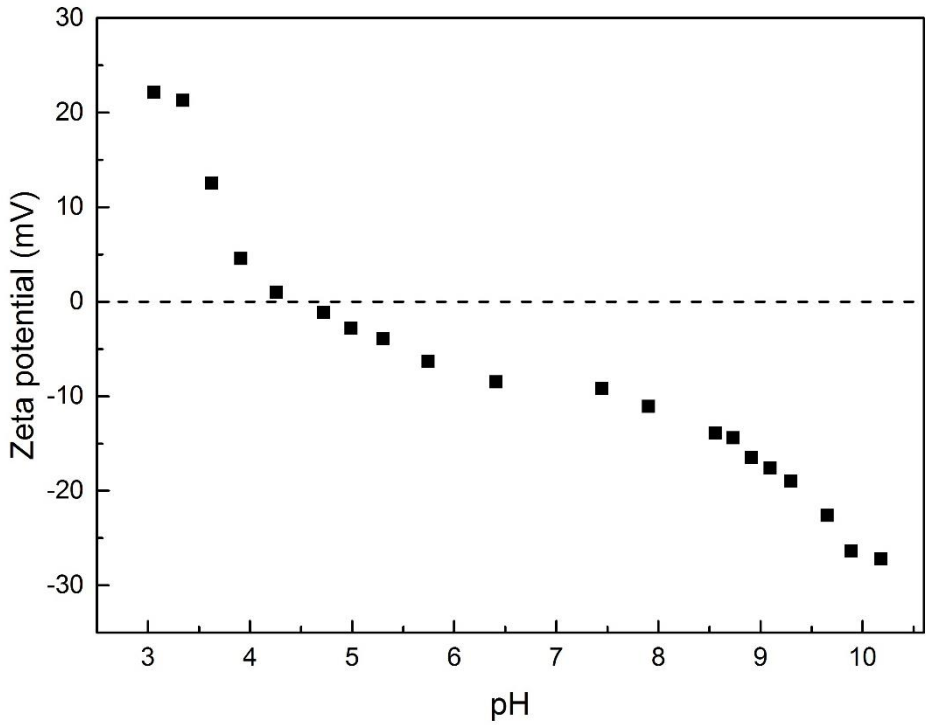

Figure F1. Zeta potential for the nanofibrous membrane.

Appendix G. Effect of the methanol pretreatment on PFOS removal efficiency

Figure G1 illustrated the PFOS removal efficiency of the membranes pretreated with (1) ultrapure water rinsing, (2) 10 ml methanol rinsing followed by ultrapure water rinsing, and (3) 50 ml methanol rinsing followed by ultrapure water rinsing. Apparently, methanol pretreatment was effective to enhance the overall PFOS removal efficiency. This improvement effect may be attributed to the removal of impurities by methanol rinsing, which may cause competition adsorption with PFOS thus reduce the removal efficiency.

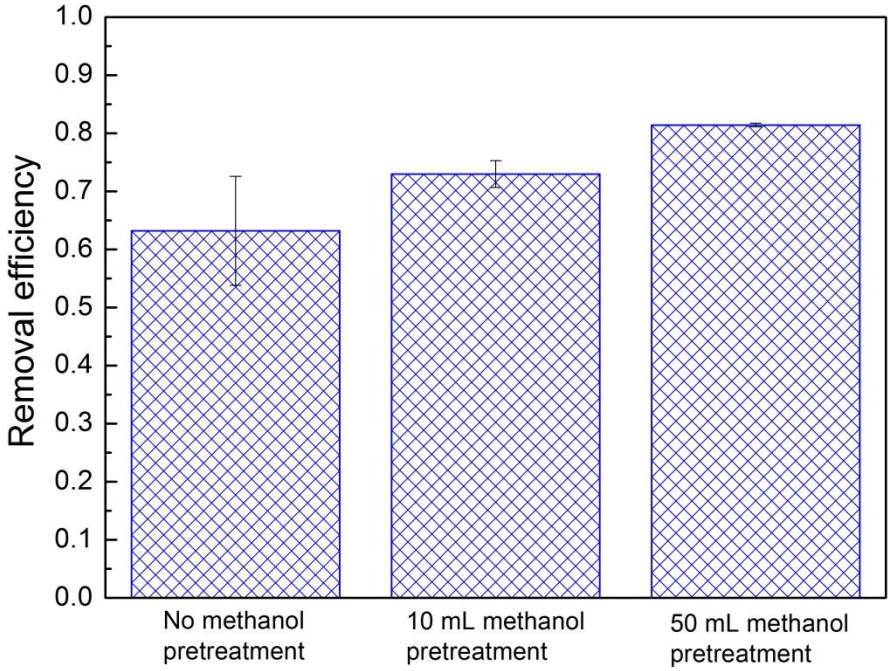

Figure G1. Effect of methanol pretreatment on PFOS removal efficiency. Experimental conditions: feed volume of 250 mL, 10 ppb PFOS, pH 7.0 and 10 mM NaCl.

References

[1] J.P. Giesy, K. Kannan, Global distribution of perfluorooctane sulfonate in wildlife, Environ. Sci. Technol., 35 (2001) 1339-1342.

[2] N. Yamashita, K. Kannan, S. Taniyasu, Y. Horii, G. Petrick, T. Gamo, A global survey of perfluorinated acids in oceans, Mar. Pollut. Bull., 51 (2005) 658-668.

[3] R. Loos, G. Locoro, S. Comero, S. Contini, D. Schwesig, F. Werres, P. Balsaa, O. Gans, S. Weiss, L. Blaha, Pan-European survey on the occurrence of selected polar organic persistent pollutants in ground water, Water Res., 44 (2010) 4115-4126.

[4] S. Wang, J. Huang, Y. Yang, Y. Hui, Y. Ge, T. Larssen, G. Yu, S. Deng, B. Wang, C. Harman, First report of a Chinese PFOS alternative overlooked for 30 years: its toxicity, persistence, and presence in the environment, Environ. Sci. Technol., 47 (2013) 10163-10170.

[5] M.M. Schultz, D.F. Barofsky, J.A. Field, Fluorinated alkyl surfactants, Environ. Eng. Sci., 20 (2003) 487-501.

[6] USEPA, Emerging Contaminants – Perfluorooctane Sulfonate (PFOS) and Perfluorooctanoic Acid (PFOA), in, 2014.

[7] OECD, Hazard Assessment of Perfluorooctane Sulfonate (PFOS) and its Salts, in: the 34th Joint Meeting of the Chemicals Committee and the Working Party on Chemicals, Pesticides and Biotechnology, Paris, November, 2002.

[8] K. Kannan, J. Koistinen, K. Beckmen, T. Evans, J.F. Gorzelany, K.J. Hansen, P.D. Jones, E. Helle, M. Nyman, J.P. Giesy, Accumulation of perfluorooctane sulfonate in marine mammals, Environ. Sci. Technol., 35 (2001) 1593-1598.

[9] C. Lau, J.L. Butenhoff, J.M. Rogers, The developmental toxicity of perfluoroalkyl acids and their derivatives, Toxicol. Appl. Pharmacol., 198 (2004) 231-241.

[10] B.L. Upham, N.D. Deocampo, B. Wurl, J.E. Trosko, Inhibition of gap junctional intercellular communication by perfluorinated fatty acids is dependent on the chain length of the fluorinated tail, Int. J. Cancer, 78 (1998) 491-495.

[11] G.L. Kennedy, J.L. Butenhoff, G.W. Olsen, J.C. O'Connor, A.M. Seacat, R.G. Perkins, L.B. Biegel, S.R. Murphy, D.G. Farrar, The toxicology of perfluorooctanoate, Crit. Rev.

Toxicol., 34 (2004) 351-384.

[12] C. Lau, K. Anitole, C. Hodes, D. Lai, A. Pfahles-Hutchens, J. Seed, Perfluoroalkyl acids: a review of monitoring and toxicological findings, Toxicol. Sci., 99 (2007) 366-394.

[13] USEPA, Perfluoralkyl Sulfonates; Significant New Use Rule in: USEPA (Ed.) OPPT-2002-0043, 2002, pp. 72854-72867.

[14] European Parliament and of the Council, Amending for the 30th time Council Directive 76/769/EEC on the approximation of the laws, regulations and administrative provisions of the Member States relating to restrictions on the marketing and use of certain dangerous substances and preparations (perfluorooctane sulfonates), in: European Parliament and of the Council (Ed.) Directive 2006/122/EC 2006.

[15] Goverment of Canada, Perfluorooctane Sulfonate and its Salts and Certain Other Compounds Regulations, in: Goverment of Canada (Ed.) SOR/2008-178, 2008.

[16] J.W. Martin, M.M. Smithwick, B.M. Braune, P.F. Hoekstra, D.C. Muir, S.A. Mabury, Identification of long-chain perfluorinated acids in biota from the Canadian Arctic, Environ. Sci. Technol., 38 (2004) 373-380.

[17] D. Skutlarek, M. Exner, H. Farber, Perfluorinated surfactants in surface and drinking waters, Environ. Sci. Pollut. Res., 13 (2006) 299.

[18] R. Loos, B.M. Gawlik, G. Locoro, E. Rimaviciute, S. Contini, G. Bidoglio, EU-wide survey of polar organic persistent pollutants in European river waters, Environ. Pollut., 157 (2009) 561-568.

[19] R. Loos, R. Carvalho, D.C. Antonio, S. Comero, G. Locoro, S. Tavazzi, B. Paracchini, M. Ghiani, T. Lettieri, L. Blaha, EU-wide monitoring survey on emerging polar organic contaminants in wastewater treatment plant effluents, Water Res., 47 (2013) 6475-6487.

[20] F.M. Hekster, P. De Voogt, A. Pijnenburg, R. Laane, Perfluoroalkylated substances: Aquatic environmental assessment, in, National Institute for Coastal and Marine Management (RIKZ). 2002.

[21] A.G. Paul, K.C. Jones, A.J. Sweetman, A first global production, emission, and environmental inventory for perfluorooctane sulfonate, Environ. Sci. Technol., 43 (2008)

386-392.

[22] B.D. Key, R.D. Howell, C.S. Criddle, Defluorination of Organofluorine Sulfur Compounds by Pseudomonas Sp. Strain D2, Environ. Sci. Technol., 32 (1998) 2283-2287.

[23] M.M. Schultz, C.P. Higgins, C.A. Huset, R.G. Luthy, D.F. Barofsky, J.A. Field, Fluorochemical Mass Flows in a Municipal Wastewater Treatment Facility†, Environ. Sci. Technol., 40 (2006) 7350-7357.

[24] J. Yu, J. Hu, S. Tanaka, S. Fujii, Perfluorooctane sulfonate (PFOS) and perfluorooctanoic acid (PFOA) in sewage treatment plants, Water Res., 43 (2009) 2399-2408.

[25] J. Cheng, C.D. Vecitis, H. Park, B.T. Mader, M.R. Hoffmann, Sonochemical degradation of perfluorooctane sulfonate (PFOS) and perfluorooctanoate (PFOA) in landfill groundwater: Environmental matrix effects, Environ. Sci. Technol., 42 (2008) 8057-8063.

[26] T. Yamamoto, Y. Noma, S.-i. Sakai, Y. Shibata, Photodegradation of Perfluorooctane Sulfonate by UV Irradiation in Water and Alkaline 2-Propanol, Environ. Sci. Technol., 41 (2007) 5660-5665.

[27] Q. Zhuo, S. Deng, B. Yang, J. Huang, G. Yu, Efficient Electrochemical Oxidation of Perfluorooctanoate Using a Ti/SnO2-Sb-Bi Anode, Environ. Sci. Technol., 45 (2011) 2973-2979.

[28] Q. Yu, R. Zhang, S. Deng, J. Huang, G. Yu, Sorption of perfluorooctane sulfonate and perfluorooctanoate on activated carbons and resin: kinetic and isotherm study, Water Res., 43 (2009) 1150-1158.

[29] S. Deng, Q. Yu, J. Huang, G. Yu, Removal of perfluorooctane sulfonate from wastewater by anion exchange resins: effects of resin properties and solution chemistry, Water Res., 44 (2010) 5188-5195.

[30] C.Y. Tang, Q.S. Fu, C.S. Criddle, J.O. Leckie, Effect of flux (transmembrane pressure) and membrane properties on fouling and rejection of reverse osmosis and nanofiltration membranes treating perfluorooctane sulfonate containing wastewater, Environ. Sci. Technol., 41 (2007) 2008-2014.

[31] E. Steinle-Darling, M. Reinhard, Nanofiltration for Trace Organic Contaminant Removal:

Structure, Solution, and Membrane Fouling Effects on the Rejection of Perfluorochemicals, Environ. Sci. Technol., 42 (2008) 5292-5297.

[32] C.Y. Tang, Q.S. Fu, A.P. Robertson, C.S. Criddle, J.O. Leckie, Use of Reverse Osmosis Membranes to Remove Perfluorooctane Sulfonate (PFOS) from Semiconductor Wastewater†, Environ. Sci. Technol., 40 (2006) 7343-7349.

[33] M. Mulder, Basic principles of membrane technology, Springer Science & Business Media, 1996.

[34] V. Thavasi, G. Singh, S. Ramakrishna, Electrospun nanofibers in energy and environmental applications, Energy Environ. Sci., 1 (2008) 205-221.

[35] K. Yoon, B.S. Hsiao, B. Chu, Functional nanofibers for environmental applications, J. Mater. Chem., 18 (2008) 5326-5334.

[36] G. Singh, D. Rana, T. Matsuura, S. Ramakrishna, R.M. Narbaitz, S. Tabe, Removal of disinfection byproducts from water by carbonized electrospun nanofibrous membranes, Sep. Purif. Technol., 74 (2010) 202-212.

[37] C.S. Ki, E.H. Gang, I.C. Um, Y.H. Park, Nanofibrous membrane of wool keratose/silk fibroin blend for heavy metal ion adsorption, J. Membr. Sci., 302 (2007) 20-26.

[38] J. Wang, K. Pan, Q. He, B. Cao, Polyacrylonitrile/polypyrrole core/shell nanofiber mat for the removal of hexavalent chromium from aqueous solution, J. Hazard. Mater., 244 (2013) 121-129.

[39] R. Ma, K. Shih, Perfluorochemicals in wastewater treatment plants and sediments in Hong Kong, Environ. Pollut., 158 (2010) 1354-1362.

[40] C. Morterra, C. Emanuel, G. Cerrato, G. Magnacca, Infrared study of some surface properties of boehmite (γ-AlO 2 H), J. Chem. Soc., Faraday Trans., 88 (1992) 339-348.

[41] Y.-H. Kim, M.S. Hwang, H.J. Kim, J.Y. Kim, Y. Lee, Infrared spectroscopy study of low-dielectric-constant fluorine-incorporated and carbon-incorporated silicon oxide films, J. Appl. Phys., 90 (2001) 3367-3370.

[42] Z. Chen, J. Hay, M. Jenkins, FTIR spectroscopic analysis of poly (ethylene terephthalate)

on crystallization, Eur. Polym. J., 48 (2012) 1586-1610.

[43] Z. Ma, M. Kotaki, T. Yong, W. He, S. Ramakrishna, Surface engineering of electrospun polyethylene terephthalate (PET) nanofibers towards development of a new material for blood vessel engineering, Biomaterials, 26 (2005) 2527-2536.

[44] C.Y. Tang, Y.-N. Kwon, J.O. Leckie, Effect of membrane chemistry and coating layer on physiochemical properties of thin film composite polyamide RO and NF membranes: II. Membrane physiochemical properties and their dependence on polyamide and coating layers, Desalination, 242 (2009) 168-182.

[45] K.P. Lee, T.C. Arnot, D. Mattia, A review of reverse osmosis membrane materials for desalination—Development to date and future potential, J. Membr. Sci., 370 (2011) 1-22.

[46] P. Zareitalabad, J. Siemens, M. Hamer, W. Amelung, Perfluorooctanoic acid (PFOA) and perfluorooctanesulfonic acid (PFOS) in surface waters, sediments, soils and wastewater - A review on concentrations and distribution coefficients, Chemosphere, 91 (2013) 725-732.

[47] F. Wang, C. Liu, K. Shih, Adsorption behavior of perfluorooctanesulfonate (PFOS) and perfluorooctanoate (PFOA) on boehmite, Chemosphere, 89 (2012) 1009-1014.

[48] G.M. Litton, T.M. Olson, Colloid deposition rates on silica bed media and artifacts related to collector surface preparation methods, Environ. Sci. Technol., 27 (1993) 185-193.

[49] C.Y. Tang, Q. Shiang Fu, D. Gao, C.S. Criddle, J.O. Leckie, Effect of solution chemistry on the adsorption of perfluorooctane sulfonate onto mineral surfaces, Water Res., 44 (2010) 2654-2662.

[50] J.G. Wijmans, R.W. Baker, The solution-diffusion model: a review, J. Membr. Sci., 107 (1995) 1-21.

[51] K.J. Hansen, H.O. Johnson, J.S. Eldridge, J.L. Butenhoff, L.A. Dick, Quantitative characterization of trace levels of PFOS and PFOA in the Tennessee River, Environ. Sci. Technol., 36 (2002) 1681-1685.

[52] D. Benford, Perfluorooctane sulfonate (PFOS), perfluorooctanoic acid (PFOA) and their salts; scientific opinion of the panel on contaminants in the food chain, EFSA J, 653 (2008) 1-131.

[53] I. Langmuir, The adsorption of gases on plane surfaces of glass, mica and platinum, J. Am. Chem. Soc., 40 (1918) 1361-1403.

[54] H. Freundlich, H.S. Hatfield, Colloid and capillary chemistry, (1926).